Assessment of the Impact of using Zeotropic Mixture on the Thermodynamic Performance of Organic Rankine Cycle Integrated Vapor Compression Refrigeration System

Ashwni
Department of Mechanical Engineering, Jamia Millia Islamia, India

Ahmad Faizan Sherwani
Department of Mechanical Engineering, Jamia Millia Islamia, India

https://doi.org/10.5109/6793668

出版情報：Evergreen. 10 (2), pp.1094-1099, 2023-06. 九州大学グリーンテクノロジー研究教育センター
バージョン：

Assessment of the Impact of using Zeotropic Mixture on the Thermodynamic Performance of Organic Rankine Cycle Integrated Vapor Compression Refrigeration System

Ashwni[1,*], Ahmad Faizan Sherwani[1]
[1]Department of Mechanical Engineering, Jamia Millia Islamia, India

*Author to whom correspondence should be addressed:
E-mail: ashwanigoyal617@gmail.com

(Received February 1, 2022; Revised May 14, 2023; accepted May 14, 2023).

Abstract: The present paper assesses the impact of the zeotropic mixture such as R245fa/ R152a, butane/R152a, and R245fa / butane on the performance of an organic Rankine cycle (ORC) - Vapor compression refrigeration (VCR) system. In this work, the system performance indicators like the coefficient of performance (COP) of the VCR subsystem and ORC-VCR system, and the exergetic efficiency of the ORC-VCR system have been evaluated. The results from the analysis indicate that the zeotropic mixture of R245fa/butane exhibits a maximum COP of 0.583 for the system and COP of 5.02 for the VCR subsystem for mixture ratios up to 0.46.

Keywords: ORC-VCR; zeotropic mixture; hydrocarbon

1. Introduction

It is estimated that the demand for electricity will rise worldwide by 70% up to the year 2030[1)]. The refrigeration sector consumes approximately 15% of the electricity[2)]. The fossil fuels such as coal, natural gas, etc. are combusted to produce electricity. The reserves of fossil fuel are limited and their combustion results in the degradation of the atmosphere[3)]. There a number of low-temperature heat sources available in an abundant amount such as industrial waste heat, solar heat, geothermal heat, etc.[4)]. However, there is a need for a cycle to exploit such sources of energy. One such cycle is the organic Rankine cycle (ORC), which is a modified form of the Rankine cycle, can be used to generate power from the above-mentioned low-temperature heat sources. ORC is simple in design, requires lower maintenance, and offers greater reliability[5)]. ORC[6)] can be used to power the refrigeration system like vapor compression refrigeration system to provide cooling. Many researchers have investigated the ORC integrated VCR system using different pure fluids. The comprehensive literature survey is given in Table 1.

The literature review done above indicates that only pure working fluids were used in the ORC-VCR system. The thermodynamic analysis of ORC-VCR using zeotropic mixtures is still to be exploited in detail by the researchers. The literature review done above indicates that only pure working fluids were used in the ORC-VCR system.

The thermodynamic analysis of ORC-VCR using zeotropic mixtures is still to be exploited in detail by the researchers. Therefore, this study investigates the thermodynamic performance of the ORC-VCR system using zeotropic mixtures.

Table 1. - Literature review

Authors	Working Fluid	Remarks/Conclusion
Aphornratana & Sriveerakul[7)]	R22 and R134a	R22 showed better thermodynamic performance than R134a
Wang et al.[8)]	R245fa	An overall COP, 0.5 of the system was achieved.
Li et al.[9)]	R290, R600, R600a, and R1270	R600 was concluded as the best working fluid
Saleh[10)]	R1270, R290, RC318, R236fa, R600a, R236ea, R600, R245fa, R1234yf, R1234ze (E)	R600 was selected as a working fluid for the ORC-VCR system.
Bu et al.[11)]	R600, R600a, R134a, R290, R123 and R245fa	R600a emerged the best as the potential working fluid in terms of expander size, COP, pressure ratios, and safety.

Molès et al.[12]	R245fa, HCFO1233zd, HFO13336mzz	The selection of HFO13336mzz for the ORC cycle and HFO13336mzz for the VCR cycle resulted in higher system efficiency.
Kim and Blanco[13]	R22, R134a, propane, R152a, R143a, R600a, R600, and ammonia	R600 and R600a were the most suitable candidate for lower ORC expander inlet pressure while R134a and R152a exhibited better thermal performance for higher ORC expander inlet pressure.
Saleh[15]	R245fa, R245ca, R236ea, R601a, R290, R600, R601, R602, RE245cb2, C5F12, R1234ze(E), RC318	R602 outplayed other working fluids in terms of overall thermal performance and environmental concerns.
Ashwni, Sherwani, and Tiwari[16]	Butane, hexane, R245fa	Hexane was found to be the most suitable fluid.
Ashwni and Sherwani[17]	Heptane, hexane, Decane, nonane, and Octane	The system performed better with the use of heptane as the working fluid.

2. Thermodynamic modelling of combined ORC-VCR system

2.1. Assumptions

The following assumptions are taken while analyzing the cycle 18).

The cycle operates under steady conditions and there is no pressure drop across connecting pipes and within the different cycle devices.

Heat losses from connecting pipes and different devices to surroundings are insignificant and thus are negligible.

Thermodynamic states at the exit of the ORC evaporator, VCR evaporator, and at the inlet of the pump are saturated ones 19).

2.2.Description of working of the cycle

ORC and VCR are the two cycles that make up this system (see figure 1). In both the ORC and VCR systems, the same zeotropic mixture is used. The combined ORC and VCR operate under the following guiding principle. The zeotropic mixture first enters the evaporator at state 1, evaporates in the evaporator to remove heat from the refrigeration chamber, and then exits the evaporator at state 2. The pressure and temperature are then raised as it enters the compressor. When the process reaches stage 3, the zeotropic mixture enters the mixer and mixes with the zeotropic mixture coming from the ORC expander. The zeotropic mixture enters the condenser at state 4 after mixing, with its whole mass flux. It leaves the condenser after that.

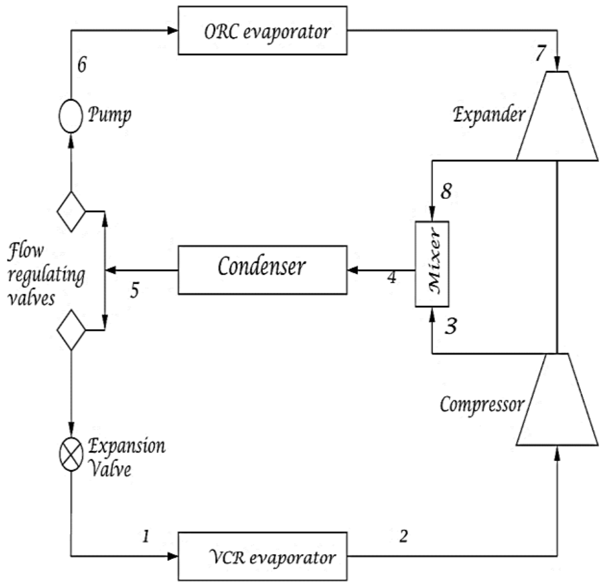

Fig. 1: Schematic diagram

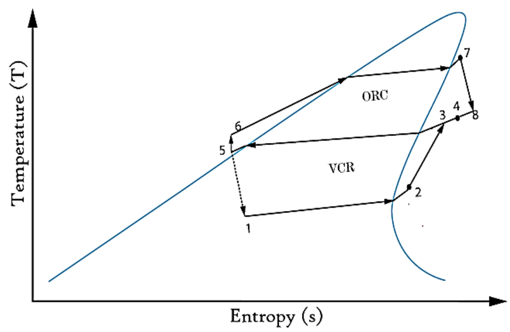

Fig. 2: T-s diagram

At state 5, the ORC zeotropic mixture enters the pump. At state 6, it leaves the pump. Once inside the ORC evaporator, it is heated to state 7 there. At state 7, it enters the expander and the expander extracts the work enough from it to run the VCR compressor. The temperature – entropy diagrams of combined ORC- VCR is shown in figure 2.

2.3.Working fluid

The choice of working fluid for the present system is governed by thermophysical properties like ozone depletion potential (ODP) 20), boiling point, chemical stability, toxicity, critical temperature (Tc) 21), critical pressure (Pc), and global warming potential (GWP) 22). The working fluids, R152a, R245fa, and butane have been chosen components of zeotropic mixtures as they show zero ODP and low GWP 23). However, butane is flammable as given in Table 2. The flammable affinity of butane is suppressed by mixing nonflammable working fluid 24).

Table 2. Thermophysical properties of working fluids

Fluid	Fluid type	ODP	GWP	T_c (^{0}C)	P_c (MPa)	NBP (^{0}C)	Safety Group
R152a	Wet	0.0	133	113.26	−24.02	A2	
Butane	Dry	0.0	20	151.98	3.79	-0.49	A3
R245fa	Dry	0.0	1050	154.1	3.65	15.14	B1

2.4. Input Data

The input values for ORC-VCR system working parameters are taken from Table 3.

Table 3. Input Data

Parameter	Value	Parameter	Value
η_p	80%	T_{2g} (K)	273
η_c	75%	T_{5f} (K)	308
η_t	80%	T_{6f} (K)	373
$\dot{m}_{orc}$	1 kg s^{-1}	T_o (K)	298

2.5.Governing equations for the cycle

Following governing equations are taken into consideration in the analysis of this cycle 25).

Mass Balance Eq.

$$\sum_{in}\dot{m} - \sum_{out}\dot{m} = \frac{d\dot{m}_{cv}}{dt} \quad (1)$$

Energy Balance Eq.

$$\sum_{in}\dot{E} - \sum_{out}\dot{E} = \frac{d\dot{E}_{cv}}{dt} \quad (2)$$

Entropy Balance Eq.

$$\sum_{in}\dot{S} - \sum_{out}\dot{S} + \dot{S}_{gen} = \frac{d\dot{S}_{cv}}{dt} \quad (3)$$

Exergy Balance Eq.

$$\sum_{in}\dot{X} - \sum_{out}\dot{X} + \dot{X}_{gen} = \frac{d\dot{X}_{cv}}{dt} \quad (4)$$

Since the steady-state, the operation is assumed, so terms on the right-hand side of Eq. (1-4) will be zero 26).

Coefficient of performance of VCR

$$COP_{vcrs} = \frac{\dot{Q}_{evap}}{\dot{W}_c} \quad (5)$$

Thermal efficiency of ORC

$$\eta_{orc} = \frac{\dot{W}_t}{\dot{Q}_b + \dot{W}_p} \quad (6)$$

COP of ORC-VCR system

$$COP_{orc-vcrs} = \eta_{orc} * COP_{vcrs} \quad (7)$$

Exergetic efficiency of ORC-VCR system

$$\eta_{ex} = \dot{EX}_u / \dot{EX}_{in} \quad (8)$$

Where $\dot{EX}_u = -\dot{Q}_{evap} * \left(1 - \left(\frac{T_o}{T_{mve}}\right)\right)$

and $\dot{EX}_{in} = \dot{Q}_b * \left(1 - \left(\frac{T_o}{T_{moe}}\right)\right)$ (9)

3. Results and Discussions

This study is carried out to analyze the thermodynamically of the system in order to evaluate the optimal mixture for considered zeotropic mixtures. The primary performance indicators are COPvcrs, COPorc-vcrs, andη_{ex}. The thermodynamic equations are coded in MATLAB 2017b with the interfacing of REFPROP 9.0.

3.1 Variation of COP_{vcrs} and $COP_{orc-vcrs}$ with mass fraction

Mass fraction refers to the first component of the zeotropic mixture. For example, for a zeotropic mixture of R245fa/R152a, mass fraction refers to the fraction of R245fa in the total mixture. Figures 6 and 7 show the variation of COP_{vcrs} and $COP_{orc-vcrs}$ with different mass fractions respectively. For butane/R152a and R245fa/R152a, as mass fraction increases from 0 to 1, both COPVCR and COPorc-vcrs first decrease to a mixture ratio of 0.7/0/.3 then again increase. For R245fa/butane, both COPVCR and COPorc-vcrs remain more or less the same up to a mass fraction of 0.46 then it decreases with an increase in mass fraction.

Both butane and R245fa are dry fluid whereas R152a is wet fluid in nature. Therefore, it can be concluded that the mixture of dry and wet fluid such as butane/R152a and R245fa/R152a does not improve either COPVCR or COPorc-vcrs. However, COP_{vcrs} and $COP_{orc-vcrs}$ can be maintained the same for a wide range of mixture ratios. The inflammability of butane can be repressed by mixing it with a non-combustible fluid, R245fa. The overall mixture is not only safe from fire hazards but also is suitable in terms of its lower GWP. The maximum values of COPvcr and COPorc-vcrs are 5.02 and 0.583 for the zeotropic mixture of R245fa/butane for up to mixture ratios of 0.46.

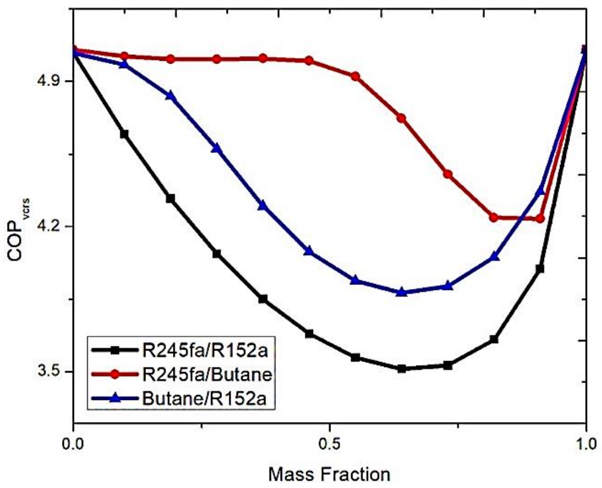

Fig. 3: COP_{vcrs} vs Mass fraction

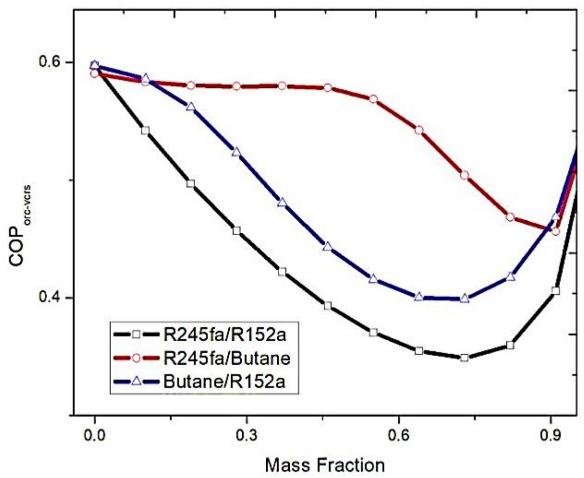

Fig. 4: $COP_{orc-vcrs}$ vs Mass fraction

3.2. Variation of η_{ex} with mass fraction

The variation of η_{ex} with the mass fraction is shown in figure 8. η_{ex} for zeotropic mixtures, namely R245fa/R152a and butane/R152a decreases with an increase in mass fraction.

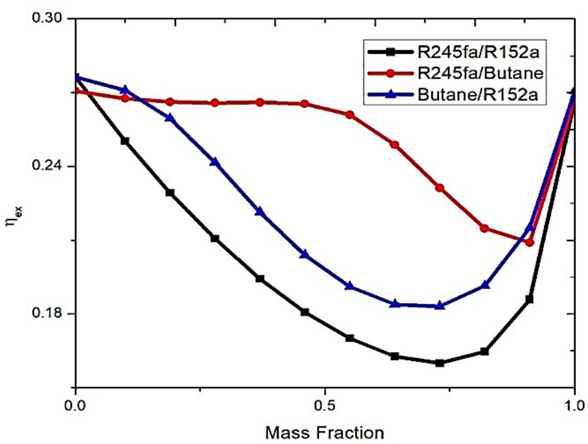

Fig. 5: η_{ex} vs Mass fraction

For R245fa/butane, exergetic efficiency more or less remains the same up to the mixture ratio of 0.46 after that it decreases. The maximum value of η_{ex} is 26.76% for a zeotropic mixture of R245fa/butane up to mixture ratios of 0.46.

3.3 The contribution of each system component in exergy destruction of the system

The contribution of each system component in the exergy destruction of the system is shown in figure 6 for the zeotropic mixture of butane/R245fa. ORC evaporator with 46%, followed by VCR evaporator with 18%, does the major contribution to the system exergy destruction.

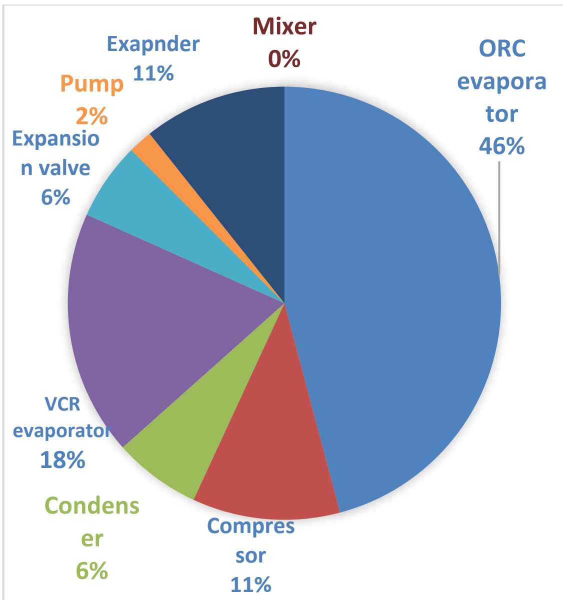

Fig. 6: Percentage contribution

4. Conclusions

The following points are being concluded from this study:

The present system is flexible in its operation and can be used in winter for electricity production whereas in summer; it can be used for refrigeration. The mixture of dry and wet fluids like R45fa/R152a and butane/R152a does not improve the thermodynamic performance of the system.

The mixing of R245fa (a non-flammable fluid) with a fluid of negligible global warming potential not only provides us with a safe fluid but also a fluid that has an overall lower GWP.

The maximum values of COPVCR and COPorc-vcrs are 5.02 and 0.583 for the zeotropic mixture of R245fa/butane for up to a mixture ratio of 0.46. The maximum value of η_{ex} is 26.76% for a zeotropic mixture of R245fa/butane up to a mixture ratio of 0.46.

ORC evaporator and VCR evaporator collectively contribute 64% to the system exergy destruction.

Nomenclature

$\dot{Q}$	Heat transfer (kW)
COP	Coefficient of performance
$\dot{W}$	Power (kW)
Greek symbols	
η	Efficiency (%)
Subscripts	
c	compressor
ex	exergy
p	pump
evap	evaporator
vcrs	vapor compression refrigeration system
orc	organic Rankine cycle

References

1) A. Goyal, and N. Kumar, " Some Experimental Studies on the Use of Tyre Pyrolysis Oil (TPO) in an Agricultural Diesel Engine," SAE Tech. Papers, 0796 (4), 1–6 (2019). https://doi.org/10.4271/2019-01-0796
2) D. Coulomb, "Refrigeration and cold chain serving the global food industry and creating a better future: two key IIR challenges for improved health and environment," Trends Food Sci. Technol.,19 (8), 413–417 (2008). https://doi.org/10.1016/j.tifs.2008.03.006.
3) B. H. Tsai, C. J. Chang, and C. H. Chang, "Elucidating the consumption and CO2 emissions of fossil fuels and low-carbon energy in the United States using Lotka–Volter," Energy, 100, 416-424 (2016).https://doi.org/10.1016/j.energy.2015.12.045.
4) A. Wahid, D. R. Mustafida, and Y. A. Husnil, "Exergy analysis of coal-fired power plants in ultra-supercritical technology versus integrated gasification combined cycle," Evergreen, 7 (1), 32–42 (2020). https://doi.org/10.5109/2740939.
5) Q. Liu, Y. Duan, and Z. Yang, "Effect of condensation temperature glide on the performance of organic Rankine cycles with zeotropic mixture working fluids," Appl. Energy, 115, 394–404 (2014).https://doi.org/10.1016/j.egypro.2019.01.383.
6) M. Sharma and R. Dev, "Review and preliminary analysis of organic Rankine cycle based on turbine inlet temperature," Evergreen, 5 (3), 22–33 (2018). https://doi.org/10.5109/1957497.
7) S. Aphornratana and T. Sriveerakul, "Analysis of a combined Rankine-vapour-compression refrigeration cycle," Energy Convers. Manag., 51 (12), 2557–2564 (2010). https://doi.org/10.1016/j.enconman.2010.04.016
8) H. Wang, R. Peterson, K. Harada, E. Miller, R. Ingram-Goble, L. Fisher, J. Yih, and C. Ward., "Performance of a combined organic Rankine cycle and vapor compression cycle for heat-activated cooling," Energy, 36 (1), 447–458 (2011). https://doi.org/10.1016/j.energy.2010.10.020
9) H. Li, X. Bu, L. Wang, Z. Long, and Y. Lian, "Hydrocarbon working fluids for a Rankine cycle powered vapor compression refrigeration system using low-grade thermal energy," Energy Build., 65, 167–172 (2013). http://dx.doi.org/10.1016/j.enbuild.2013.06.012
10) B. Saleh, "Parametric and working fluid analysis of a combined organic Rankine-vapor compression refrigeration system activated by low-grade thermal energy," J. Adv. Res., 7 (5), 651–660 (2016). http://dx.doi.org/10.1016/j.jare.2016.06.006.
11) X. Bu, L. Wang, and H. Li, "Working fluids selection for fishing boats waste heat powered organic Rankine-vapor compression ice maker," Heat Mass Transf., 50, (10), 1479–1485 (2014). https://doi.org/10.1007/s00231-014-1350-0.
12) F. Molés, J. Navarro-Esbrí, B. Peris, A. Mota-Babiloni, and K. Kontomaris, "Thermodynamic analysis of a combined organic Rankine cycle and vapor compression cycle system activated with low-temperature heat sources using low GWP fluids," Appl. Therm. Eng., 87, 444–453 (2015). http://dx.doi.org/10.1016/j.applthermaleng.2015.04.083.
13) K. H. Kim and H. Perez-Blanco, "Performance analysis of a combined organic Rankine cycle and vapor compression cycle for power and refrigeration cogeneration," Appl. Therm. Eng., 91, 964–974 (2015). 10.1016/j.applthermaleng.2015.04.062.
14) M. T. Nasir and K. C. Kim, "Working fluids selection and parametric optimization of an Organic Rankine Cycle coupled Vapor Compression Cycle (ORC-VCC) for air conditioning using low-grade heat," Energy Build., 129, 378–395 (2016). http://dx.doi.org/doi:10.1016/j.enbuild.2016.07.068.
15) B. Saleh, "Energy and exergy analysis of an integrated organic Rankine cycle-vapor compression refrigeration system," Appl. Therm. Eng., 141, 697–710(2018).https://doi.org/10.1016/j.applthermaleng.2018.06.018
16) Ashwni, A. F. Sherwani, and D. Tiwari, "Exergy, economic and environmental analysis of organic Rankine cycle based vapor compression refrigeration system," Int. J. Refrig., 126, 259–271 (2021).https://doi.org/10.1016/j.ijrefrig.2021.02.005.
17) Ashwni and A. F. Sherwani, "Thermodynamic analysis of hybrid heat source driven organic Rankine cycle integrated vapor-compression refrigeration system," Int. J. Refrig., (2021). https://doi.org/10.1016/j.ijrefrig.2021.05.006.
18) R. A. Rouf, M. A. Hakim Khan, K. M. Ariful Kabir, and B. B. Saha, "Energy management and heat

storage for solar adsorption cooling," Evergreen, 3 (2), 1–10 (2016). https://doi.org/10.5109/1800866.
19) Ashwni, A. F. Sherwani, D. Tiwari, and A. Kumar, "Sensitivity analysis and multi-objective optimization of organic Rankine cycle integrated with vapor compression refrigeration system," Energy Sources, Part A Recover. Util. Environ. Eff., (2021).https://doi.org/10.1080/15567036.2021.1916132.
20) M. T. Kibria, M. A. Islam, B. B. Saha, T. Nakagawa, and S. Mizuno, "Assessment of environmental impact for air-conditioning systems in Japan using HFC based refrigerants," Evergreen, 6 (3), 246–253 (2019). https://doi.org/10.5109/2349301.
21) O. Badr, S. D. Probert, and P. W. O'Callaghan, "Selecting a working fluid for a Rankine-cycle engine," Appl. Energy, 21 (1), 1–42 (1985). https://doi.org/10.1016/0306-2619(85)90072-8.
22) S. Y. Wu, H. Yang, L. Xiao, and C. Li, "Comparative Investigation on Thermo-economic Performance between ORC and LiBr Absorption Refrigerating Cycle in Waste Heat Recovery," Energy Procedia, 105, 1446–1453 (2017). https://doi.org/10.1016/j.egypro.2017.03.425.
23) V. Maizza and A. Maizza, "Unconventional working fluids in organic Rankine-cycles for waste energy recovery systems," Appl. Therm. Eng., 21 (3), 381–390 (2001). https://doi.org/10.1016/S1359-4311(00)00044-2.
24) Ashwni, A. F. Sherwani, and D. Tiwari, "Thermodynamic analysis of simple and modified organic Rankine cycle and vapor compression refrigeration (ORC–VCR) systems," Environ. Prog. Sustain. Energy, 40 (3) (2020). https://doi.org/10.1002/ep.13577.
25) U. Perera, N. Takata, T. Miyazaki, Y. Higashi, and K. Thu, "The exergy investigation of a mechanical vapor compression chiller for cooling using r410a," Evergreen, 8 (1), 213–220 (2021). https://doi.org/10.5109/4372281.
26) Ashwni, and Ahmad Faizan Sherwani, "Advanced Exergy Analysis of Renewable Heat Source Driven ORC-VCR System," Mater. Today Proc., (2022). https://doi.org/10.1016/j.matpr.2021.12.440